2021 43rd Annual International Conference of the
IEEE Engineering in Medicine & Biology Society (EMBC)
Oct 31 - Nov 4, 2021. Virtual Conference

Isolating Transcutaneous Spinal Cord Stimulation Artifact to Identify Motor Response during Walking*

Kamyar Momeni, Rakesh Pilkar, Manikandan Ravi, and Gail F. Forrest, *Member, IEEE*

***Abstract* — The objective of this investigation was to demonstrate the applicability of a custom-developed EMD-Notch filtering algorithm to isolate the scTS-induced artifact from sEMG signals during walking in an individual with motor-incomplete SCI. Overall, the EMD-Notch filtering algorithm provides an effective approach to isolate the scTS artifact, extract the sEMG data, and further study the modulation of the spinal neuronal networks during dynamic activities.**

***Clinical Relevance*— This investigation will help with the modification of individualized scTS parameters to achieve task-specific neuromodulatory effects.**

I. Introduction

Non-invasive spinal cord transcutaneous stimulation (scTS) is applied to one or multiple spinal segments and has been shown to depolarize large-diameter afferent fibers of the posterior roots in humans to neuromodulate the physiological state of the spinal cord [1]–[4].

Recovery of motor function for individuals with incomplete spinal cord injury (iSCI) is often studied by utilizing surface electromyography (sEMG), a sensitive technique for analyzing motor activity by recording electrical activity of muscles; however, the overpowering presence of scTS-induced electrical stimulation artifact in the sEMG signal limits the ability to measure motor response during different neuromodulation techniques.

Recent advances in biomedical signal processing have yielded specific algorithms that successfully remove electrical stimulation artifacts from sEMG signals recorded during neuromuscular stimulation [5]–[7]. Our group has previously shown the effectiveness of a custom-developed computational algorithm, utilizing empirical mode decomposition (EMD) and notch filtering, to remove the neuromuscular electrical stimulation artifact from sEMG recordings during standing [8]. The objective of this investigation was to demonstrate the applicability of our custom-developed EMD-Notch filtering algorithm to isolate the scTS-induced artifact from sEMG signals during walking in an individual with motor-incomplete SCI. We expect to observe a strong correlation between the sEMG signals (without using scTS) and the ones extracted by using the EMD-Notch algorithm from recordings contaminated by scTS artifact.

II. Methodology

A. Participants

An individual with motor-incomplete SCI and an able bodied (AB) control were recruited to participate in this study (Table I). Prior to their participation, both individuals provided written informed consent to the study procedures, which were approved by Kessler Foundation's Institutional Review Board. The individual with SCI has a neurological level of injury at C8, according to International Standards for Neurological Classification of SCI (ISNCSCI). The AB participant had no history of neurological or orthopedic disorders.

TABLE I. Participant Demographics

	Gender	*Age (yrs.)*	*Height (cm)*	*Weight (kg)*	*TSI* [a] *(yrs.)*	*AIS* [b]
SCI	female	47	170	54	3	D
AB	male	21	174	78	–	–

a. Time since Injury; b. American Spinal Injury Association Impairment Scale

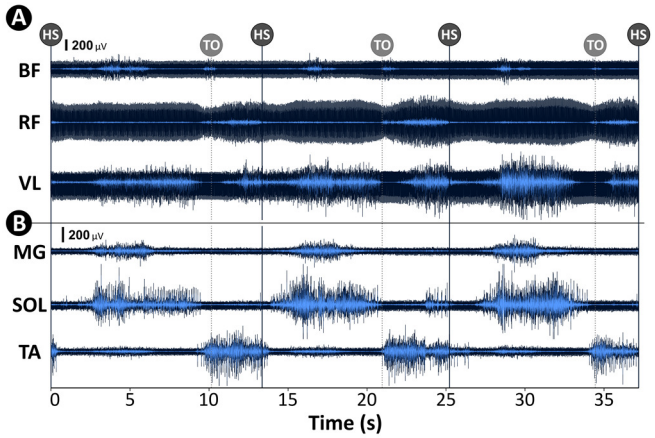

Figure 1. sEMG signals from left upper leg (A) and lower leg (B) muscles of SCI participant before any signal processing (dark blue). The overpowering presence of scTS artifact is visible in contrast with the sEMG signals that are processed (light blue) with the proposed EMD-Notch filtering algorithm in this work.

B. Spinal Cord Transcutaneous Stimulation (scTS)

scTS was delivered by using an electrical stimulator (BioStim-5, Cosyma, Russia). One self-adhesive round (2.5 cm) stimulating electrode (STIMEX, Schwamedico GmbH, Germany) was placed over the midline of spinous processes as cathode and a pair of rectangular anode electrodes (8x13 cm) were placed over the iliac crests. scTS was delivered at three spinal levels, simultaneously: between spinous processes T1-T2, T11-T12, and L1-L2, with 1 ms monophasic square-wave pulses at a frequency of 30 Hz, filled with a carrier frequency

*Research supported by Tim Reynolds Foundation.

G. F. Forrest is with Reynolds Center for Spinal Stimulation, Kessler Foundation, West Orange, NJ 07052 USA (corresponding author: gforrest @ KesslerFoundation.org).

K. Momeni and M. Ravi are with Reynolds Center for Spinal Stimulation, Kessler Foundation, West Orange, NJ 07052 USA.

R. Pilkar is with Center for Mobility and Rehabilitation Engineering Research, Kessler Foundation, West Orange, NJ 07052 USA.

of 10 kHz. Stimulation intensities for T1-T2, T11-T12, and L1-L2 were set at 25, 50, and 50 mA, respectively.

C. Data Collection

Both participants were asked to walk across a 10-meter walkway at a self-selected speed, as previously reported [4], [9]. The SCI participant used canes and tonic scTS was delivered throughout the walking trial.

sEMG data were collected at 10 kHz using the 16-channel MA400 systems (Motion Lab Systems, Baton Rouge, LA, USA). Bipolar sEMG electrodes, with two 12 mm disks and an inter-electrode distance of 17 mm, were placed on the following muscles bilaterally: gluteus maximus (GM), medial bicep femoris (BF), rectus femoris (RF), vastus lateralis (VL), medial gastrocnemius (MG), soleus (SOL), and tibialis anterior (TA). Electrode placement protocol has been explained in further detail elsewhere [10], [11]. Ground electrodes were placed on the clavicles for providing a common reference. Prior to electrode placement, skin was prepared by shaving, cleansing with alcohol, and lightly abrading. Preparations and electrode placements were performed by the same examiner throughout the study to ensure repeatability and consistency.

Kinematic data (Motion Analysis Corporation, Santa Rosa, CA) were collected at 60Hz using reflective markers, placed on anatomical landmarks throughout the body according to the Helen-Hayes marker set. Data from at least 3 gait cycles in a trial were used.

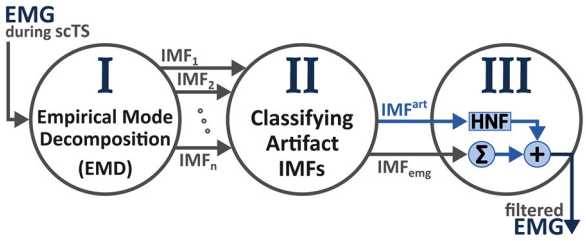

Figure 2. Schematic illustration of the three-stage process implemented in the custom-developed EMD-Notch Filtering algorithm [8] that isolates scTS artifact from sEMG signals. (HNF: Harmonic Notch Filters)

D. Data Processing

The sEMG signals were band-pass filtered between 20 to 450 Hz using a 4th order, zero-lag Butterworth filter. Next, data were processed using our custom-developed computational algorithm [6], [8]. Fig. 2 illustrates the stages of the process implemented in the algorithm to isolate and extract the scTS artifact from the sEMG data. The three stages are described below:

Stage I – Empirical Mode Decomposition (EMD): The process of *Sifting* is used to identify intrinsic oscillatory modes in the signal; when repeatedly applied, the signal is decomposed into its intrinsic mode functions (IMFs) allowing the instantaneous characteristics to be observed with better resolution than the traditional methods of isolating stimulation artifacts from the sEMG signal [6]. At the end of the sifting process what remains is a residual signal (r_n), from which no further IMFs can be retrieved. The outcome of the sifting process is the decomposition of the original signal into a finite number of IMFs and a residual signal (r_n) (Fig. 3).

Stage II – Classifying Artifact IMFs: IMFs generated during Stage I are assessed for their standard deviations (SD). The amplitude of the stimulation artifact is generally higher in magnitude compared to physiological muscle response by a factor of 3 [12]. The difference in magnitude is utilized to detect and classify the *artifact IMFs* (IMF_{art}), which are most affected by scTS artifact (Fig. 4). Remaining IMFs are referred to as IMF_{emg}.

Stage III – Applying Notch-Filters: the sEMG signals collected during scTS contain a stimulation artifact similar to the stimulation frequency and its harmonics. Therefore, a series of notch filters is applied on each IMF_{art}. Notch filters are 2nd order, zero-lag Butterworth band-stop filters with cut-off frequencies equivalent to the stimulation frequency and its subsequent harmonics and a spread of less than ±6 Hz.

All the IMF_{emg} and notch-filtered IMF_{art} were added together to construct the filtered signal. sEMG signals for 3 gait cycles were averaged and the full-wave rectified linear-envelopes were compared between SCI and AB participants by calculating the normalized cross-correlation coefficients for each muscle between participants, as well as agonist/antagonist pairs of BF/RF, BF/VL, TA/MG, and TA/SOL within each participant.

III. Results

The sEMG signals collected during walking were processed with the EMD-Notch filtering algorithm; however, for the purpose of demonstration, results from only left side are shown in this paper.

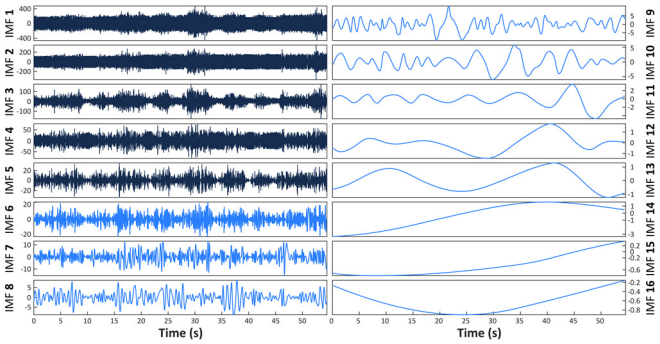

Figure 3. sEMG signal from left vastus lateralis is decomposed into 16 intrinsic mode functions (IMFs) via *Stage I* of the EMD-Notch filtering algorithm. IMFs 1-5 are detected as artifact modes [8].

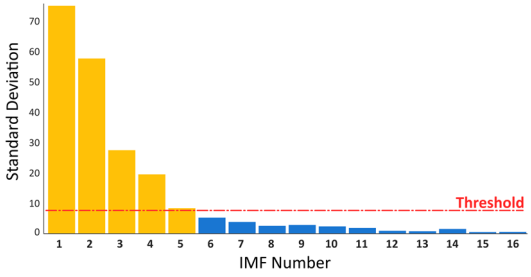

Figure 4. Stage II: classifying artifact IMFs (yellow bars, IMFs 1-5) based on a threshold determined by standard deviation.

A. *Isolating scTS Artifact in One Muscle*

In stage I, the algorithm decomposed the sEMG signals into several IMFs (e.g., 16 IMFs for left VL, as shown in Fig. 3). Stage II classified IMFs 1-5 as artifact IMFs due to the presence of high magnitude scTS artifact. In stage III, a series of notch filters were applied to the artifact IMFs and the output signal of the algorithm was generated. As seen in Fig. 5, the EMD-Notch algorithm was able to reconstruct the sEMG signal after isolating and removing the scTS-induced artifact.

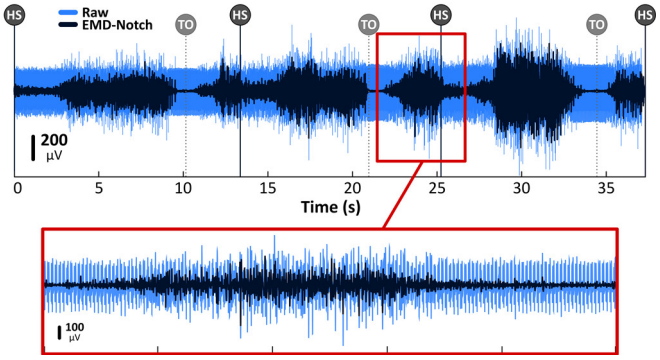

Figure 5. sEMG signal from left vastus lateralis before (light blue) and after (dark blue) EMD-Notch filtering during overground walking. Gait events are marked as HS (heel strike) and TO (toe-off). A 5-second segment is enlarged to better illustrate the details.

Fig. 5 demonstrates the effectiveness of the EMD-Notch algorithm in reconstructing the sEMG signal in one muscle (i.e., left VL). Data show the bursts of muscle activity throughout four consecutive gait cycles. The Fourier transforms of the raw and filtered sEMG signals also show that the algorithm isolated and removed the scTS artifact while retaining the 20-400 Hz spectrum of sEMG data (Fig. 6).

B. *Comparing Muscle Activity Patterns during Walking*

Filtered and full-wave rectified sEMG activity for three consecutive gait cycles, during walking at a self-selected speed, are shown in Fig. 7A for SCI (with scTS) and the average of three gait cycles is shown in Fig. 7B for both SCI and AB participants. All gait cycles are time-normalized (0-100%). The filtered, lower-limb sEMG signals for the SCI participant demonstrate a distinct and repetitive profile with reciprocal agonist/antagonist activity patterns during gait. Calculated cross-correlation coefficients between participants range from 0.70 to 0.96 for left muscles (Fig. 7B). Coefficient values for muscle pairs are presented in Table 2.

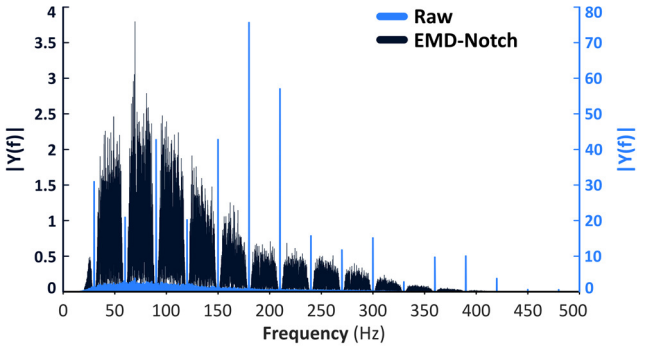

Figure 6. Fast Fourier transforms of the sEMG signal from left vastus lateralis before (black, right Y-axis) and after (blue, left Y-axis) EMD-Notch filtering during overground walking.

TABLE II. CROSS-CORRELATION VALUES FOR AGONIST AND ANTAGONIST MUSCLE PAIRS

	BF / RF		*BF / VL*		*TA / MG*		*TA / SOL*	
	r	*% lag*	*r*	*% lag*	*r*	*% lag*	*r*	*% lag*
AB	0.73	+25	0.79	0	0.63	+38	0.69	+45
SCI	0.79	-55	0.83	-6	0.90	+48	0.80	+49

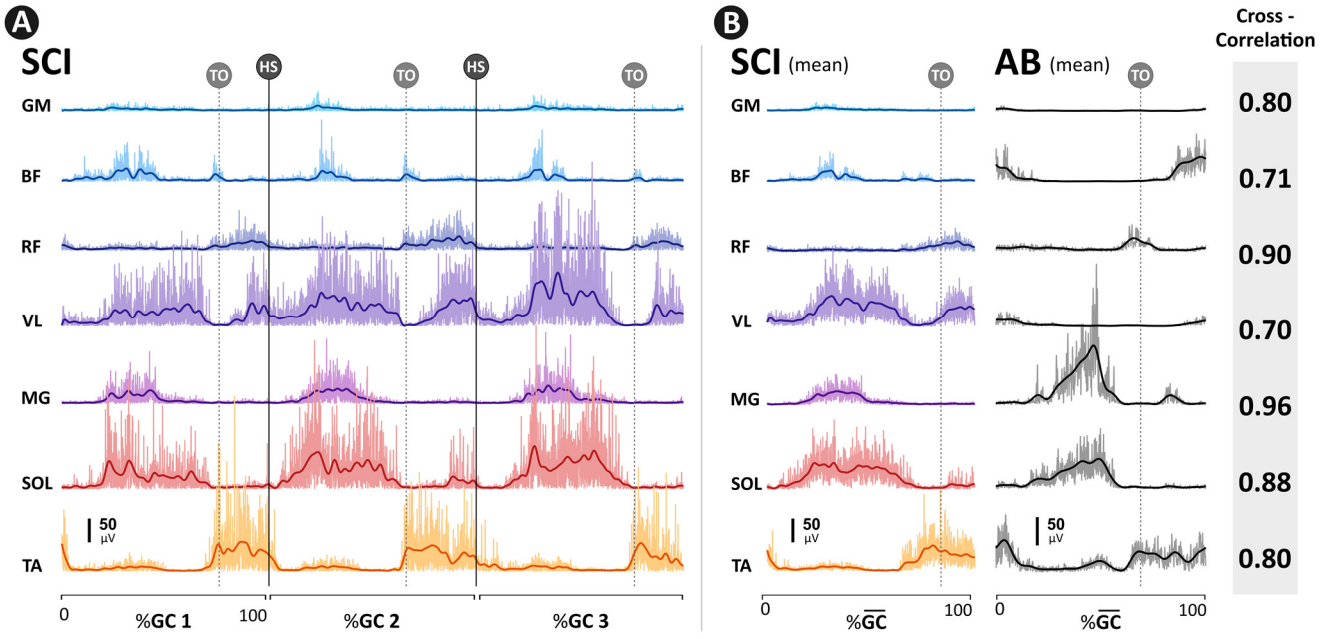

Figure 7. (A) Full-wave rectified, filtered sEMG signals (overlaid with a linear envelope) from lower extremity muscles of participant with SCI during overground walking with scTS (left muscles, 3 gait cycles). sEMG signals from SCI have been processed using the EMD-Notch filtering algorithm. All gait cycles are time-normalized and gait events are marked by HS (heel strike) and TO (toe-off). (B) Mean sEMG signals of three gait cycles (overlaid with a linear envelope) for left muscles of SCI and AB. Cross-correlation coefficients were calculated by comparing mean sEMG signals for each muscle across participants.

IV. Discussion

Previous studies have shown that combining electrical stimulation with various forms of rehabilitation trainings (e.g., stand retraining, exoskeleton, etc.) may lead to significant functional recovery for individuals with SCI [3], [11], [13]–[15]. However, one major challenge in studying the physiological effects of electrical stimulation on muscle activities is isolating and removing the stimulation artifact present in recorded sEMG signals [6], [16], [17]. We have previously developed and validated a robust signal processing and computational algorithm [6], [8] to extract sEMG signals during neuromuscular electrical stimulation (NMES). Current study is an improvement to our previous work by demonstrating: i) the successful translation of our algorithms from a static (standing) to a complex dynamic condition (walking); and ii) the effectiveness of the algorithm in isolating stimulation artifact induced by multi-site scTS (as opposed to single-channel NMES) to examine the physiological effects of scTS on multi-muscle activations during walking overground.

When examining the physiological aspects of scTS during overground walking, the muscles proximal to the most caudal scTS site (BF, RF, VL) displayed higher levels of scTS-induced stimulation artifact, relative to distal muscles (Fig. 1). However, all recorded sEMG signals required utilizing the EMD-Notch algorithm to extract meaningful sEMG data. To evaluate the reciprocal muscle activity patters in lower extremity [15], we calculated cross-correlation coefficients by correlating the SCI participant's filtered sEMG signals with those of the AB. The lag percentages for muscle pairs show the similarity in reciprocal gait patters between participants, with the exception of BF/RF pair. Our findings further determine the applicability of our algorithm in isolating the scTS-induced artifact from sEMG during walking.

A common limitation of the basic EMD algorithm is mode mixing, which results in a mode to remain mixed in multiple IMFs. To minimize this effect, we implemented the use of notch filters in the EMD-Notch algorithm. However, a widely accepted solution has been proposed in the literature: noise assisted Ensemble EMD [18], which is a computationally intensive process and requires further optimization for its application in processing sEMG signals recorded while electrical stimulation is applied.

Another limitation of our approach is that applying scTS to multiple spinal sites with different stimulation parameters affects the sEMG recordings with an aggregated effect. The EMD-Notch filtering algorithm requires further development to be able to isolate scTS artifact produced by multiple frequencies and shapes of stimulation.

In conclusion, our algorithm provides an avenue to study the effects of scTS on muscle activity patterns that were previously masked by the overwhelming magnitudes of the scTS artifact. Once processed, the artifact-free sEMG can provide a wide range of sEMG outcomes, such as burst duration, time-to-peak, mean frequency, etc. This will allow for a better understanding of the physiological effects scTS may have on a potentially neuromodulated system. Overall, the EMD-Notch filtering algorithm provides an effective approach to isolate the scTS-induced artifact, extract the sEMG data, and further study the modulation of the spinal neural networks during dynamic activities, such as walking.

References

[1] Y. Gerasimenko, R. Gorodnichev, T. Moshonkina, D. Sayenko, P. Gad, and V. Reggie Edgerton, "Transcutaneous electrical spinal-cord stimulation in humans," *Ann. Phys. Rehabil. Med.*, vol. 58, no. 4, pp. 225–231, Sep. 2015.

[2] C. Angeli, V. R. Edgerton, Y. Gerasimenko, and S. Harkema, "Reply: No dawn yet of a new age in spinal cord rehabilitation," *Brain*, vol. 138, no. 7, pp. e363–e364, 2015.

[3] F. Zhang *et al.*, "Cervical Spinal Cord Transcutaneous Stimulation Improves Upper Extremity and Hand Function in People with Complete Tetraplegia: A Case Study," *IEEE Trans. Neural Syst. Rehabil. Eng.*, vol. 28, no. 12, pp. 3167–3174, Dec. 2020.

[4] A. Ramanujam *et al.*, "Neuromuscular response to transcutaneous spinal stimulation during overground walking," in *Program No. 571.04. 2019 Neuroscience Meeting Planner. Chicago, IL: Society for Neuroscience, 2019. Online.*, 2019.

[5] R. Pilkar, A. Ramanujam, E. Garbarini, and G. F. Forrest, "Validation of empirical mode decomposition combined with notch filtering to extract electrical stimulation artifact from surface electromyograms during functional electrical stimulation," in *Proceedings of the Annual International Conference of the IEEE Engineering in Medicine and Biology Society, EMBS*, 2016, vol. 2016-Octob, pp. 1733–1736.

[6] R. B. Pilkar, M. Yarossi, and G. Forrest, "Empirical mode decomposition as a tool to remove the function Electrical stimulation artifact from surface electromyograms: Preliminary investigation," *Proc. Annu. Int. Conf. IEEE Eng. Med. Biol. Soc. EMBS*, vol. 2012, pp. 1847–1850, 2012.

[7] Y. Zhou *et al.*, "A Data-Driven Volitional EMG Extraction Algorithm During Functional Electrical Stimulation With Time Variant Parameters.," *IEEE Trans. Neural Syst. Rehabil. Eng.*, vol. 28, no. 5, pp. 1069–1080, May 2020.

[8] R. Pilkar *et al.*, "Application of Empirical Mode Decomposition Combined with Notch Filtering for Interpretation of Surface Electromyograms during Functional Electrical Stimulation," *IEEE Trans. Neural Syst. Rehabil. Eng.*, vol. 25, no. 8, pp. 1268–1277, 2017.

[9] A. Ramanujam *et al.*, "Center of mass adaptations and its interaction between the trunk and lower-extremity during exoskeleton walking," *2019 Wearable Robot. Assoc. Conf. WearRAcon 2019*, pp. 57–62, 2019.

[10] F. P. Kendall *et al.*, *Muscles: Testing and Function, with Posture and Pain*, vol. 53, no. 9. 2013.

[11] K. Momeni, A. Ramanujam, E. L. Garbarini, and G. F. Forrest, "Multi-muscle electrical stimulation and stand training: Effects on standing.," *J. Spinal Cord Med.*, vol. 42, no. 3, pp. 378–386, May 2019.

[12] M. Knaflitz, M. Knaflitz, R. Merletti, and R. Merletti, "Suppression of Simulation Artifacts from Myoelectric-Evoked Potential Recordings," *IEEE Trans. Biomed. Eng.*, vol. 35, no. 9, pp. 758–763, 1988.

[13] E. Rejc, C. A. Angeli, N. Bryant, and S. J. Harkema, "Effects of Stand and Step Training with Epidural Stimulation on Motor Function for Standing in Chronic Complete Paraplegics," *J. Neurotrauma*, vol. 34, no. 9, pp. 1787–1802, 2017.

[14] F. B. Wagner *et al.*, "Targeted neurotechnology restores walking in humans with spinal cord injury.," *Nature*, vol. 563, no. 7729, pp. 65–71, 2018.

[15] K. Momeni, A. Ramanujam, M. Ravi, E. Garbarini, and G. F. Forrest, "Effects of Multi-Muscle Electrical Stimulation and Stand Training on Stepping for an Individual With SCI," *Front. Hum. Neurosci.*, vol. 14, Sep. 2020.

[16] D. T. O'Keeffe, G. M. Lyons, A. E. Donnelly, and C. A. Byrne, "Stimulus artifact removal using a software-based two-stage peak detection algorithm.," *J. Neurosci. Methods*, vol. 109, no. 2, pp. 137–45, Aug. 2001.

[17] T. Wichmann and A. Devergnas, "A novel device to suppress electrical stimulus artifacts in electrophysiological experiments," *J. Neurosci. Methods*, vol. 201, no. 1, pp. 1–8, Sep. 2011.

[18] Z. Wu and N. E. Huang, "Ensemble empirical mode decomposition: A noise-assisted data analysis method," *Adv. Adapt. Data Anal.*, vol. 1, no. 1, pp. 1–41, Jan. 2009.